Supporting Information

Sn-Doped Co-P-Based Trifunctional Electrocatalysts for Accelerating Water Splitting and Hydrogen Generation Concurrent with Ethylene Glycol Electrooxidation

Tanu Bagaria,[1,2] Sougata Saha,[3] Swapan K. Pati,[3]* Anustup Sadhu,[1]* Bharati Debnath[2]*

[1]*Department of Chemistry, Techno India University, Salt Lake Sector V, Kolkata 700091, India*

[2]*Research Institute for Sustainable Energy (RISE), Center for Research and Education in Science and Technology (TCG-CREST), Salt Lake, 700091 Kolkata, India*

[3]*Theoretical Sciences Unit, School of Advanced Materials (SAMat), Jawaharlal Nehru Centre for Advanced Scientific Research, Jakkur, Bangalore 560064, India*

*Email: pati@jncasr.ac.in; anustup.s@technoindiaeducation.com; bharati.debnath@tcgcrest.org

1. Faradic Efficiency Calculation

Faradaic efficiency was determined by using the formula given below:

$$\text{Faradic Efficiency (F.E.)} = n_{(experimental)} / n_{(theoretical)}$$

where, $n_{(experimental)}$ is the amount of gas evolved during the water splitting reaction, measured by Gas chromatography (GC) (G3545A 8890A GC System, Agilent Technologies).

$n_{(theoretical)}$ was calculated as follows:

$$n_{(theoretical)} = (I * t) / (n*F)$$

where, I = Current (A); t = Time (in second); n = moles of H_2 generated per mole of H_2O molecule; F = Faraday's constant (96485 C mol^{-1}).

2. Electrochemical Active Surface Area (ECSA) Calculation

The ECSA was calculated using the formula given below:

$$ECSA = (A \times C_{dl})/C_s \text{ where,}$$

A = geometric area (in cm^2) = 0.5 cm^2

C_s = Specific capacitance = 40 μF cm^{-2}

$$ECSA = (A \times C_{dl})/40$$

ECSA is proportional to double layer capacitance (C_{dl}). Cyclic voltammograms (CVs) with various scan rates (from 120 - 200 mV s^{-1} with a step of 20 mV s^{-1}) in non-faradaic potential region (from 0.1 – 0.2 V vs RHE) was measured to find C_{dl}. All currents measured in this potential region are considered to be related with double-layer charging. C_{dl} was calculated by linear fitting of the plot obtained by plotting voltage measured at $\Delta j_{0.13}$ against the scan rate. In this work, 40 μF cm^{-2} is used as the C_s for calculating ECSA.

$$|\Delta j_{013}| = \text{anodic } j_{0.13} - \text{cathodic } j_{0.13}$$

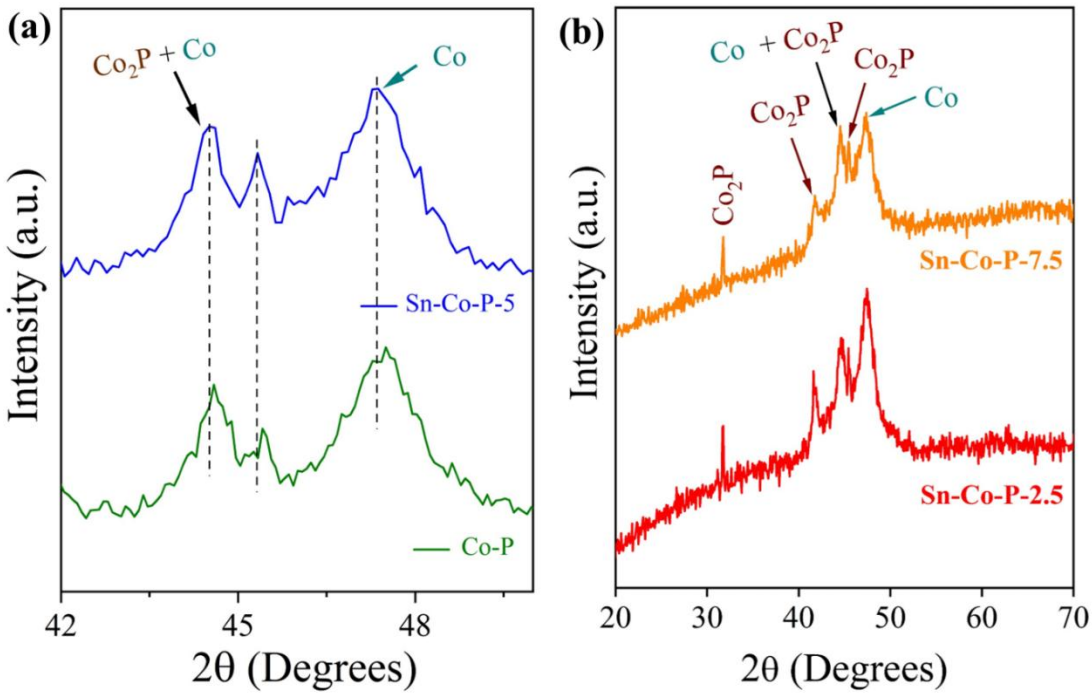

Figure S1. (a) Zoom XRD patterns of Sn undoped (Co-P) and Sn-doped catalyst (Sn-Co-P-5); (b) XRD patterns of Sn-Co-P-2.5 and Sn-Co-P-7.5.

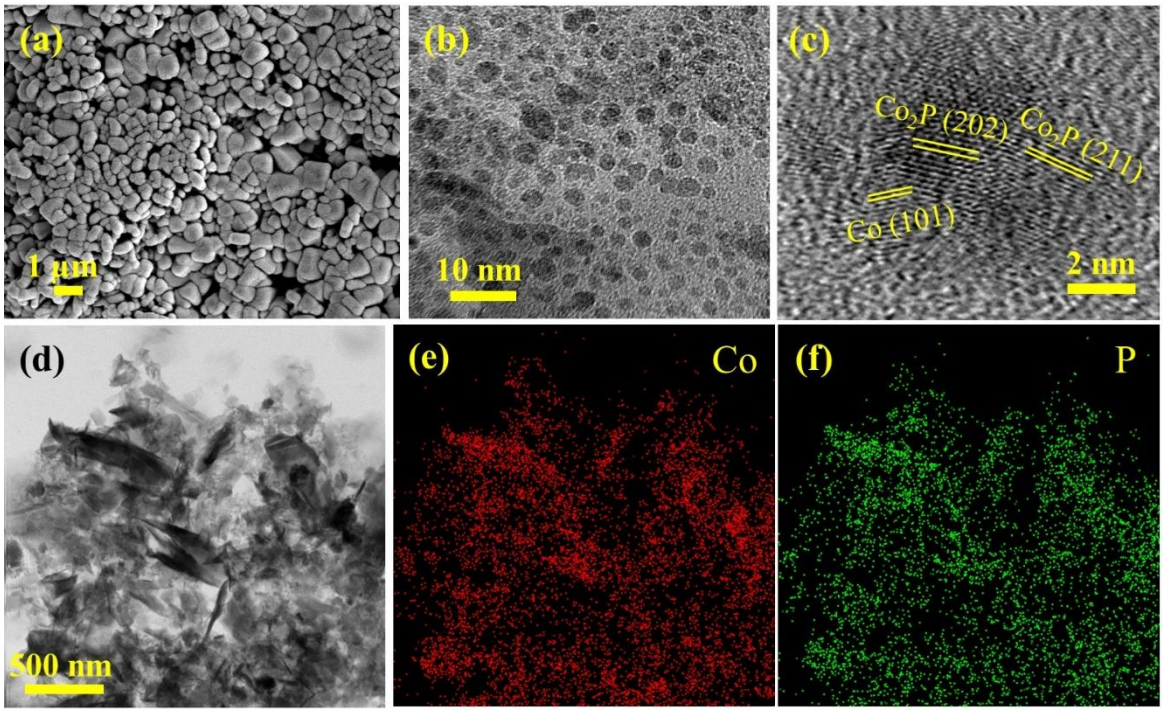

Figure S2. (a) Top view SEM, (b) TEM, and (c) HRTEM images of Co-P. (d-f) HAADF-STEM and the corresponding EDS element colour mapping for (e) Co and (f) P.

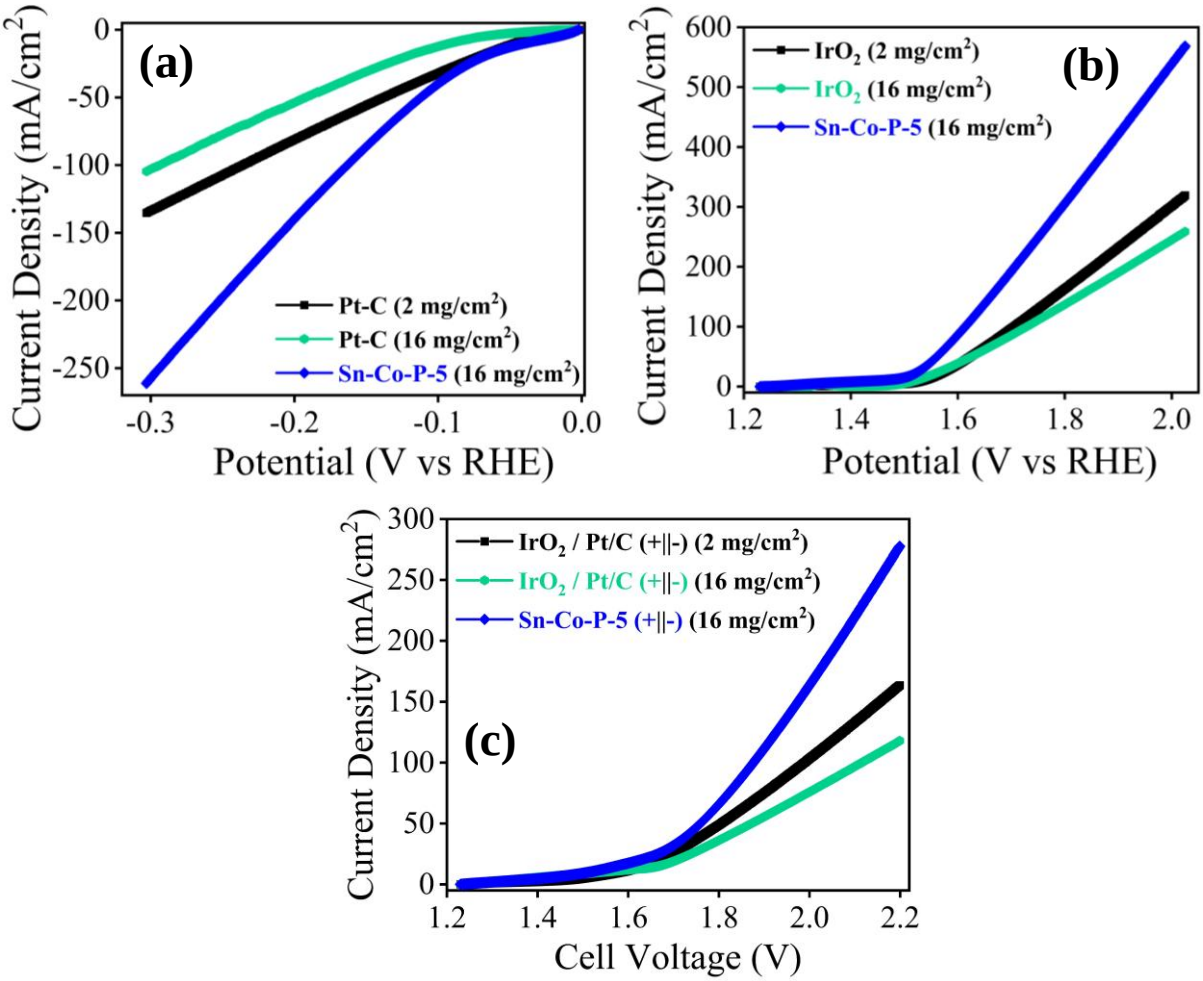

Figure S3. Polarization curves for (a) HER, (b) OER, and (c) overall water splitting in 1 M KOH, comparing the best-performing designed catalysts at identical loadings with commercial catalysts (Pt/C and IrO_2), along with commercial catalysts tested at their most used loading (2 mg/cm^2).

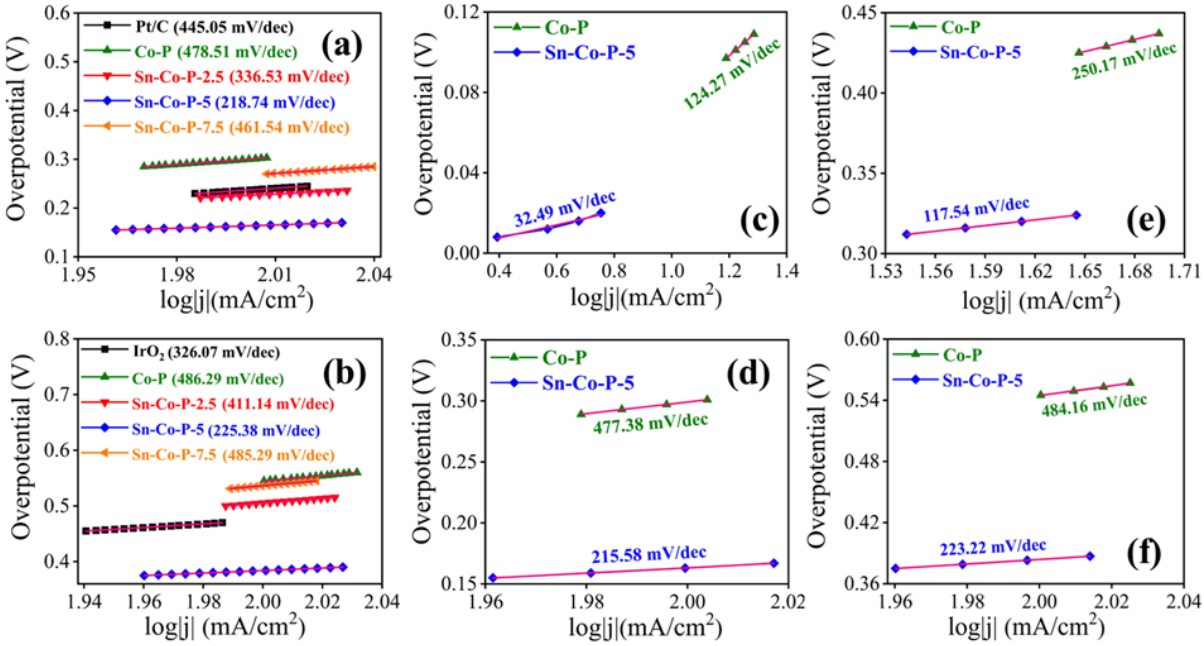

Figure S4. Tafel plots for (a) HER and (b) OER in higher potential region using LSV; Tafel plots for HER using potentiostatic technique in (c) lower and (d) higher potential region; Tafel plots for OER using potentiostatic technique in (e) lower and (f) higher potential region.

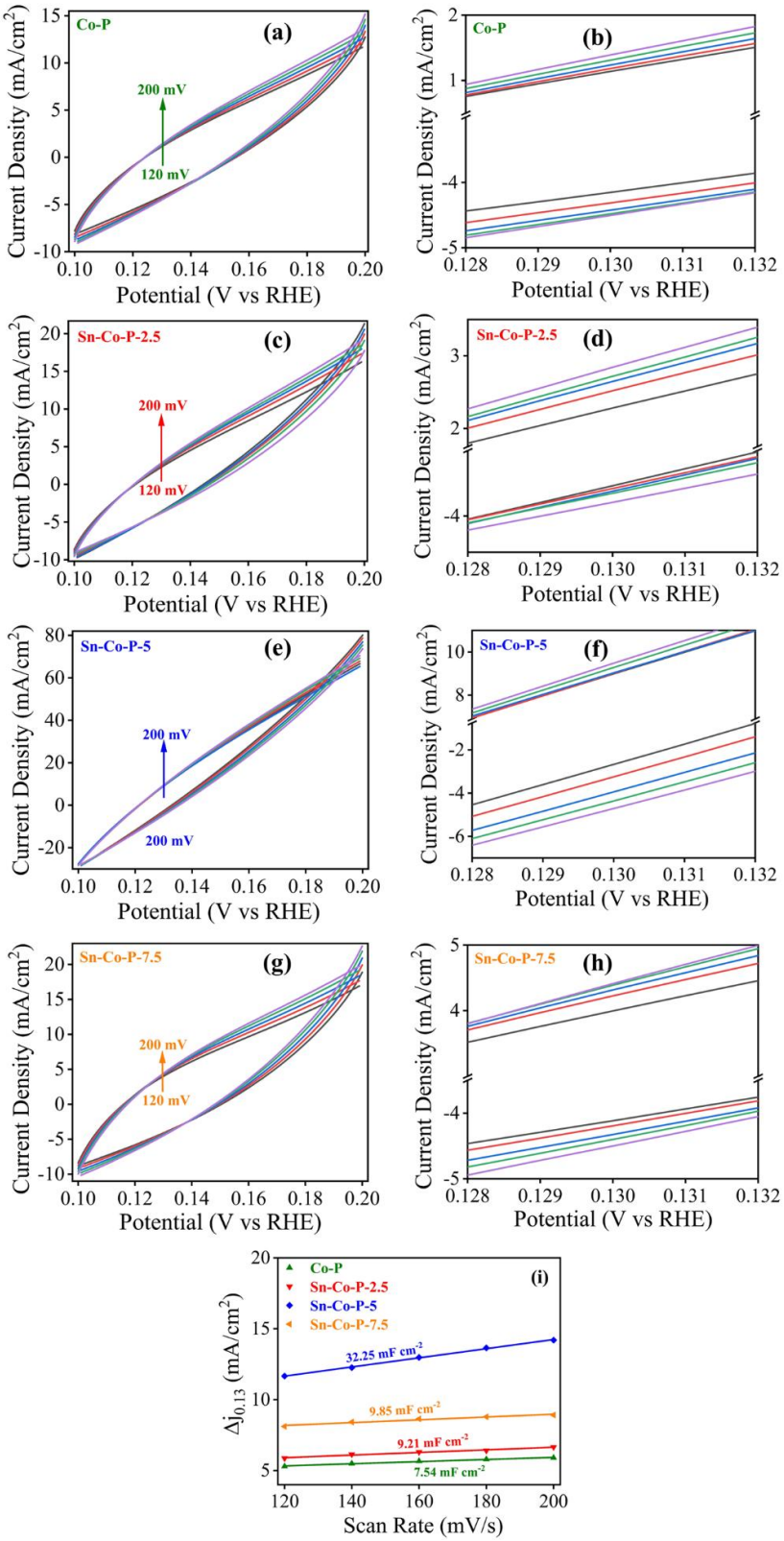

Figure S5. CV curves in the non-faradaic potential range for (a) Co-P, (c) Sn-Co-P-2.5, (e) Sn-Co-P-5, (g) Sn-Co-P-7.5; and Zoom CV curves for (b) Co-P, (d) Sn-Co-P-2.5, (f) Sn-Co-P-5, and (h) Sn-Co-P-7.5; (i) Current density versus scan rate plots for Co-P and Sn-doped Co-P.

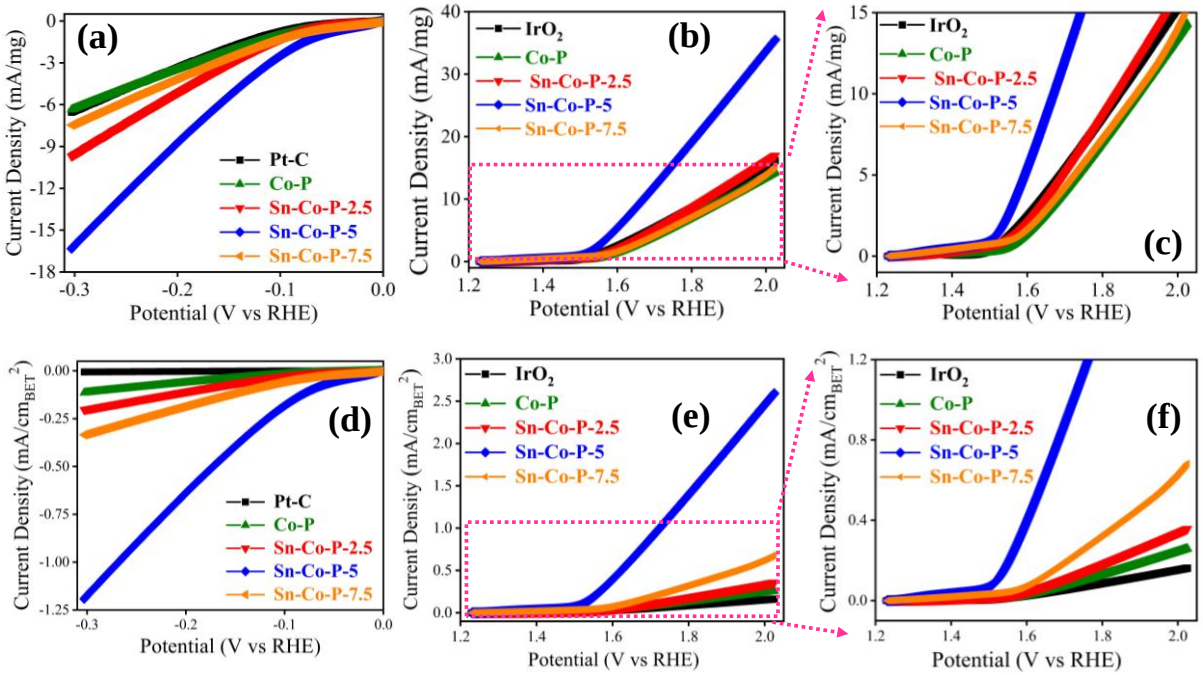

Figure S6. Mass activity for (a) HER, (b) OER and (c) Zoom image of (b); BET-normalized LSV curves for (d) HER, (e) OER and (f) Zoom image of (e).

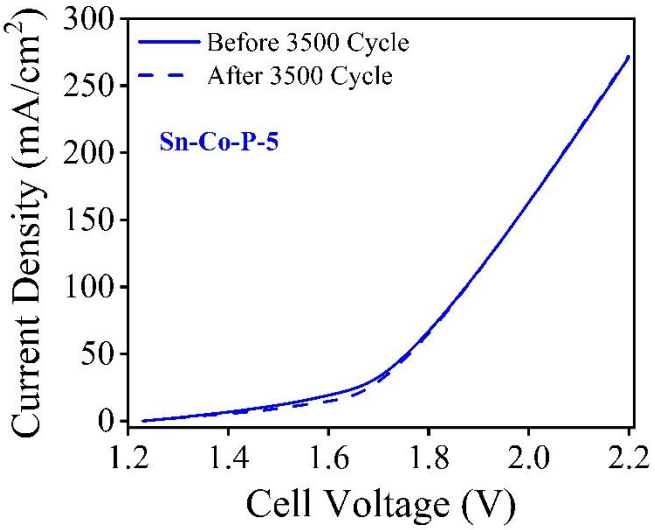

Figure S7. Cyclic stability assessment for Sn-Co-P-5 for overall water splitting at 25 °C in 1 M KOH.

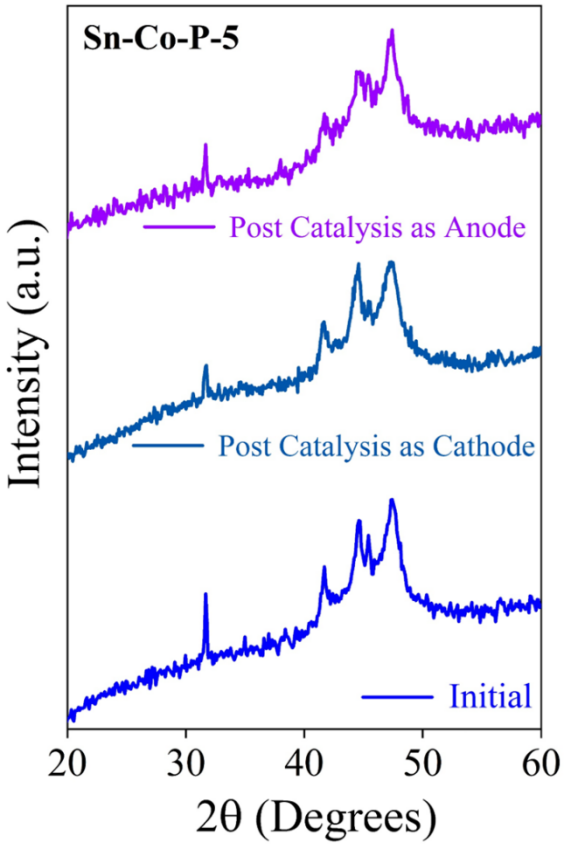

Figure S8. XRD patterns of Sn-Co-P-5 after overall water splitting at the anode and cathode sides in 1 M KOH.

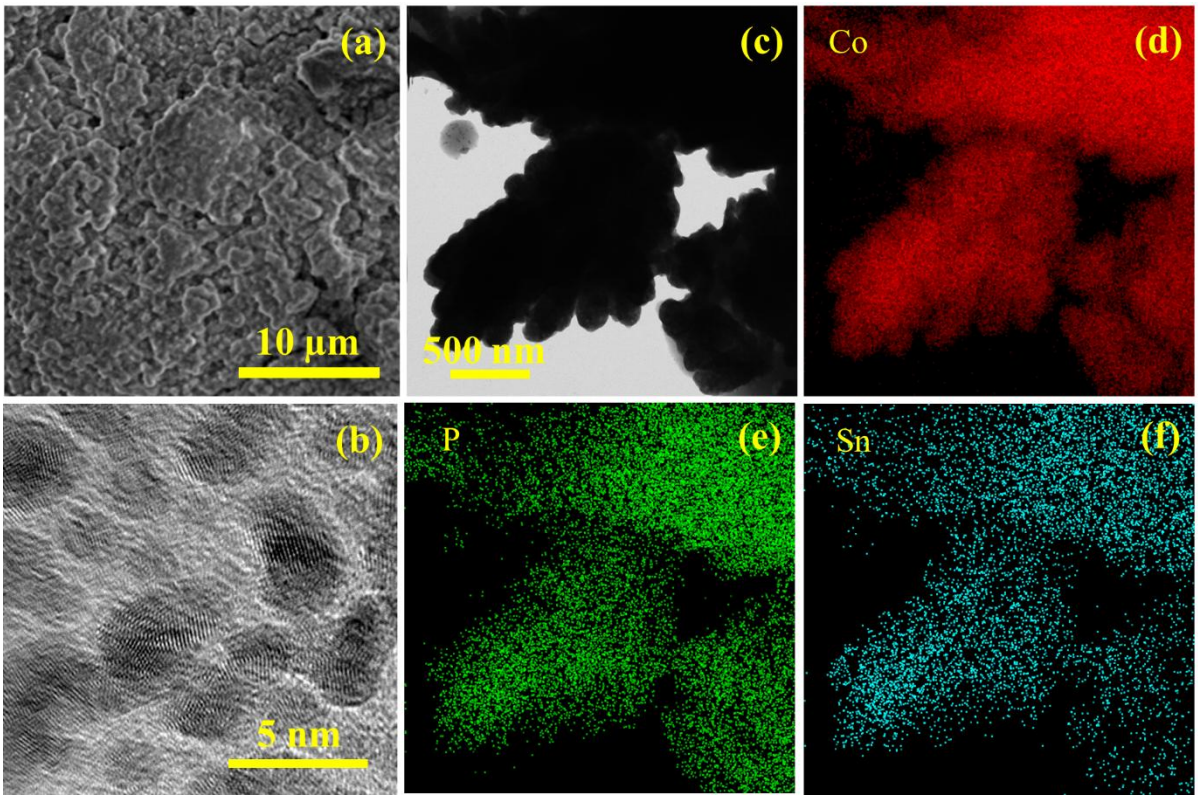

Figure S9. (a) Top view SEM, (b) HRTEM images of Sn-Co-P-5 after overall catalysis at the cathode side. (c-f) HAADF-STEM and the corresponding EDS element color mapping for (d) Co, (e) P, and (f) Sn of Sn-Co-P-5.

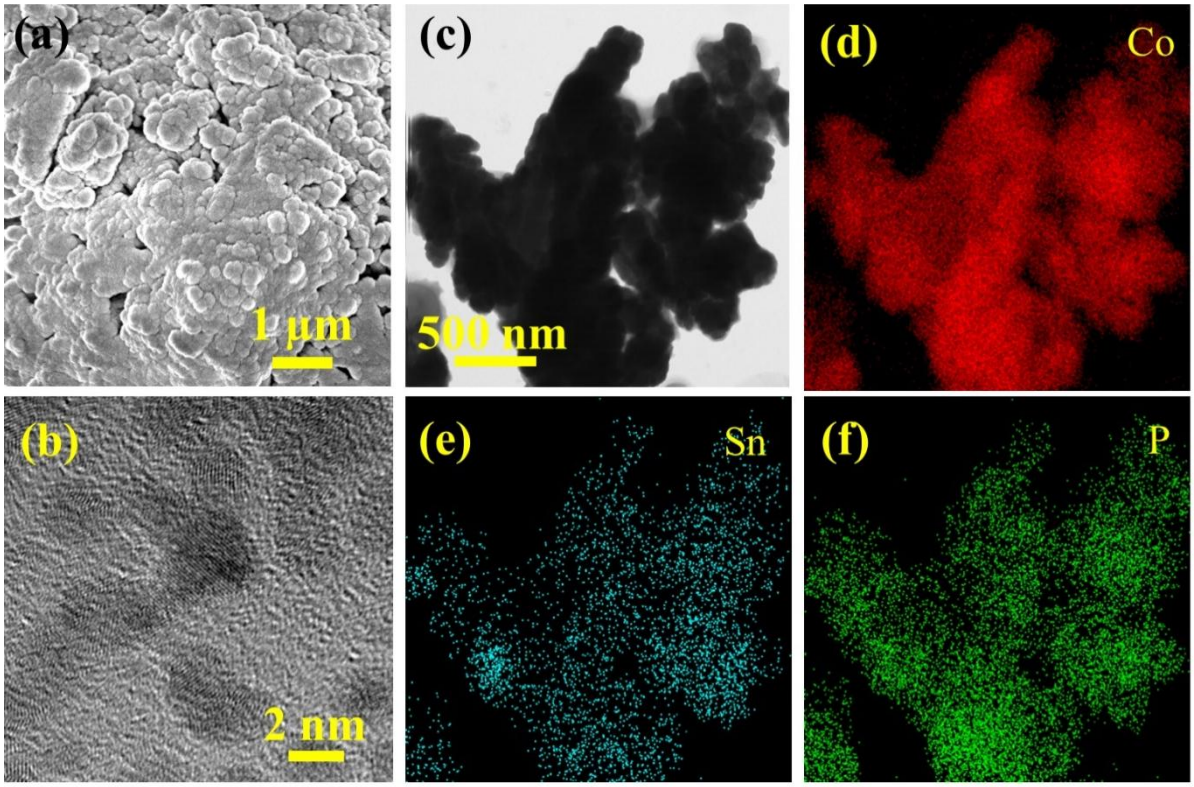

Figure S10. (a) Top view SEM, (b) HRTEM images of Sn-Co-P-5 after overall catalysis at the anode side. (c-f) HAADF-STEM and the corresponding EDS element color mapping for (d) Co, (e) P, and (f) Sn of Sn-Co-P-5.

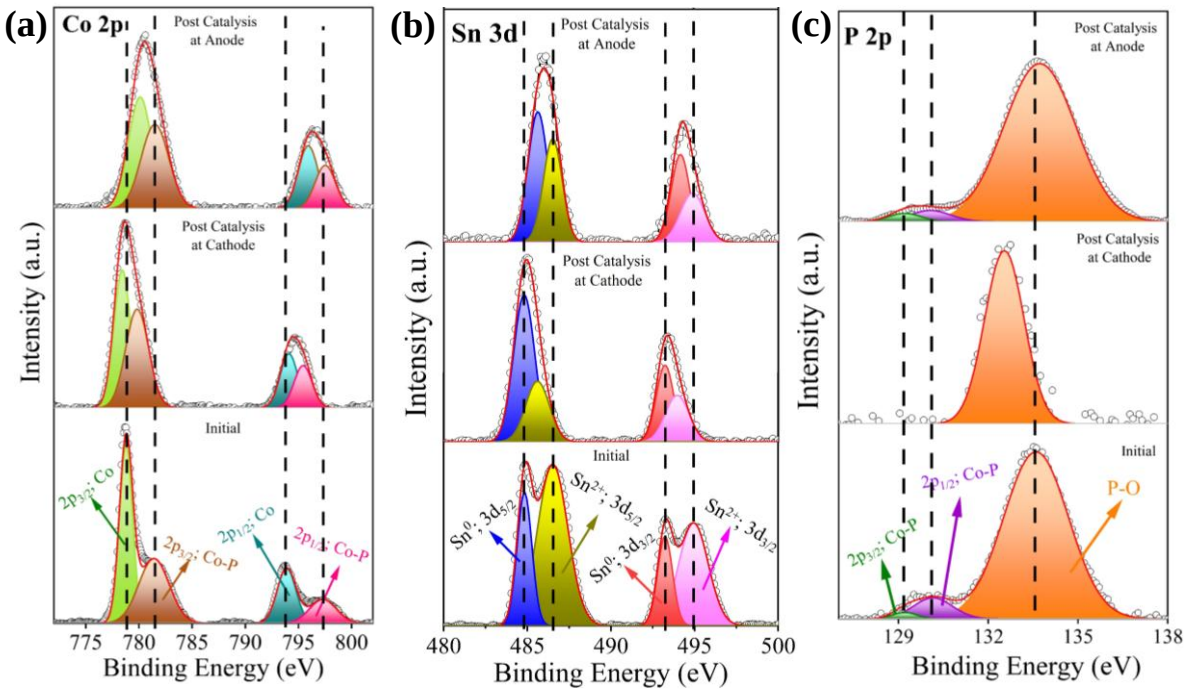

Figure S11. High-resolution XPS spectra of Sn-Co-P-5 fresh and after overall water splitting at the cathode and anode (a) Co 2p, (b) Sn 3d and (c) P 2p in 1 M KOH.

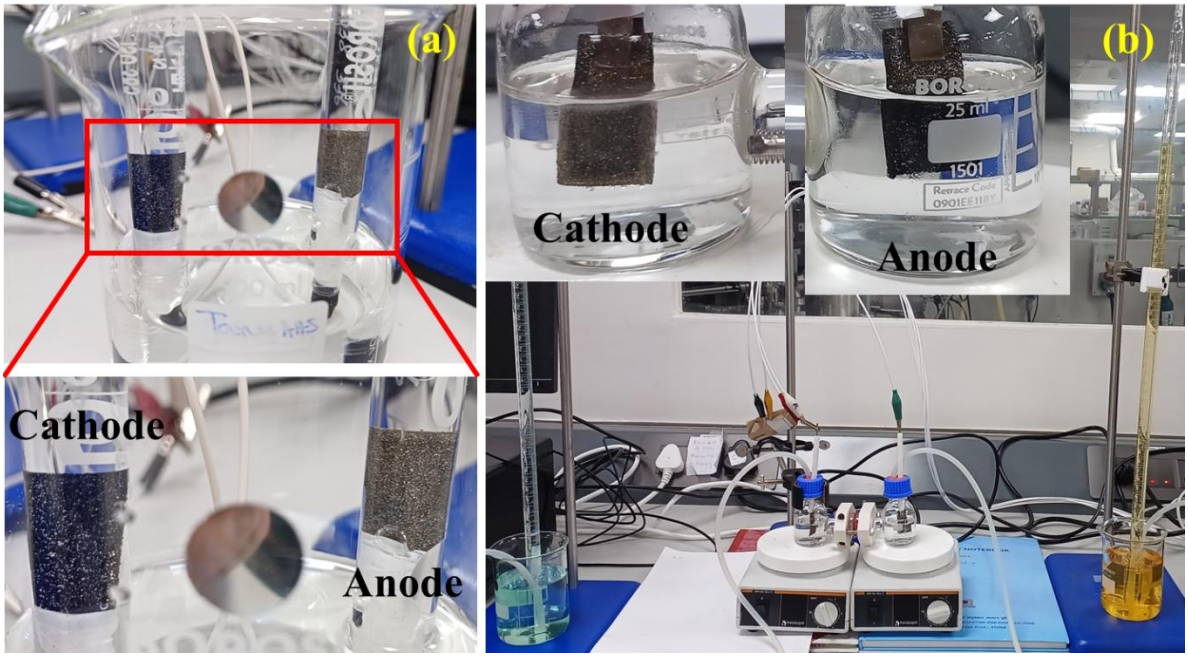

Figure S12. (a) Digital photograph of H_2 and O_2 bubbles evolving from the electrodes during electrolysis via water displacement method; (b) Digital photography of gas measurement setup to calculate Faradic efficiency using H-cell.

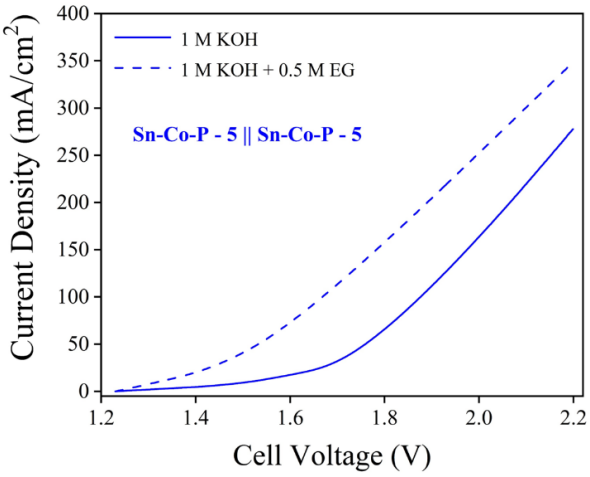

Figure S13. Comparison of the polarization curve of Sn-Co-P-5 with and without 0.5 M EG in 1 M KOH.

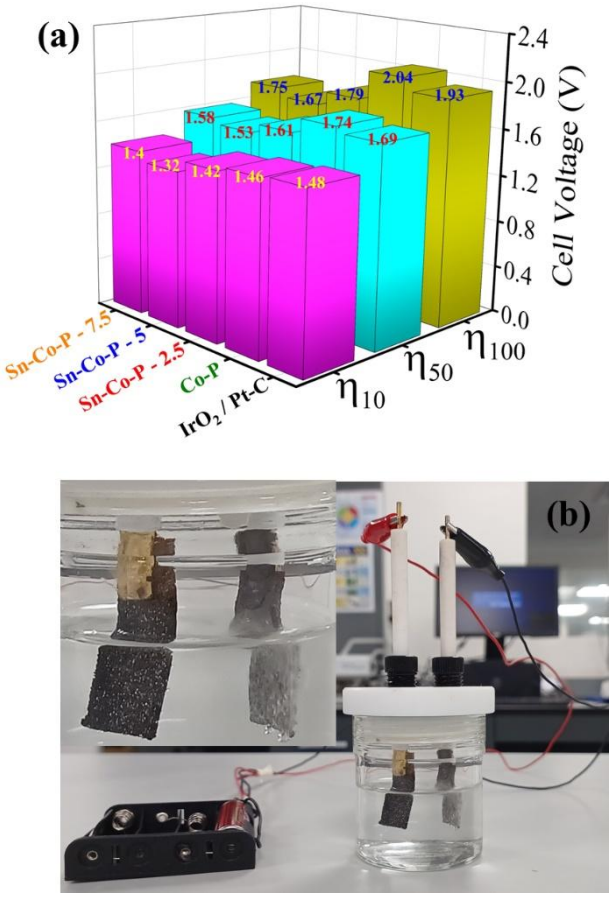

Figure S14. (a) Corresponding cell voltages at the current densities of 10, 50, and 100 mA cm^{-2} using 0.5 M EG in 1 M KOH at 25 °C for commercial catalysts and designed catalysts; (b) Photograph of a device for EG oxidation along with HER driven by a single 1.5 V AA battery.

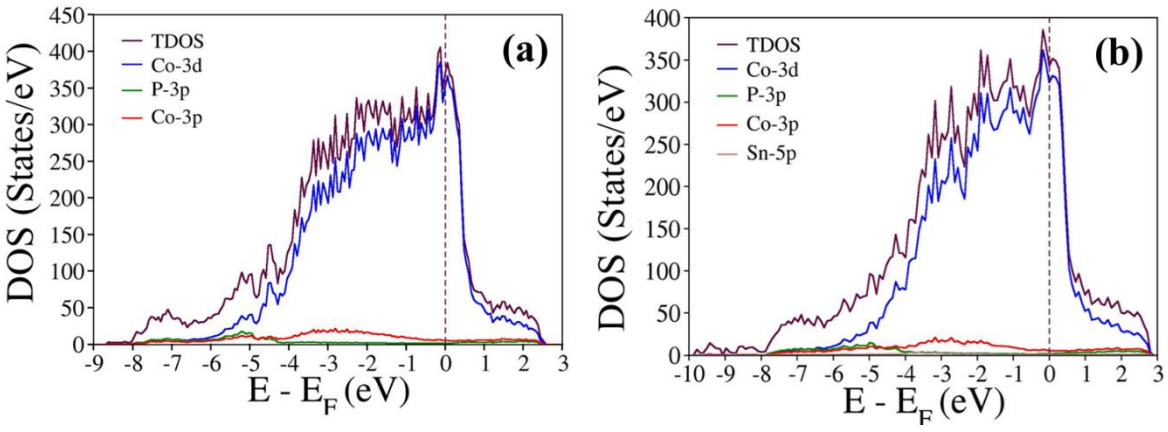

Figure S15. DOS plots of (a) Co-P and (b) Sn-Co-P.

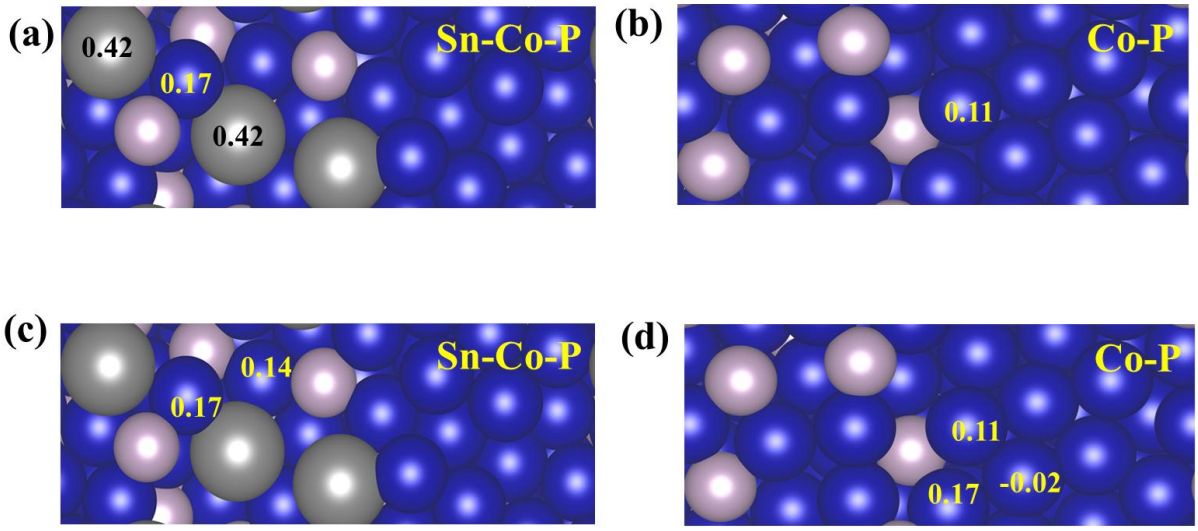

Figure S16. Bader charge distribution on the optimized surface of Sn-Co-P (comprising 77 Co, 3 Sn and 16 P atoms) and Co-P (comprising 8o Co and 16 P atoms) focusing on (a,b) the active site of H_2O adsorption and (c,d) the active sites H adsorption.

Table S1. The compositions of the catalysts were obtained using EDAX and AAS techniques.

Sample Name	Expected Co: Sn Ratio	Actual Co: Sn Ratio from AAS	Co: Sn Ratio from EDAX	(Co + Sn): P Ratio from EDAX
Sn-Co-P-2.5	$Co_{0.975}$: $Sn_{0.025}$	$Co_{0.98}$: $Sn_{0.02}$	$Co_{0.984}$: $Sn_{0.016}$	$(Co + Sn)_1$: $P_{0.72}$
Sn-Co-P-5	$Co_{0.95}$: $Sn_{0.05}$	$Co_{0.94}$: $Sn_{0.06}$	$Co_{0.955}$: $Sn_{0.045}$	$(Co + Sn)_1$: $P_{0.65}$
Sn-Co-P-7.5	$Co_{0.925}$: $Sn_{0.075}$	$Co_{0.922}$: $Sn_{0.078}$	$Co_{0.926}$: $Sn_{0.074}$	$(Co + Sn)_1$: $P_{0.63}$

Table S2. Fitting impedance parameters for the equivalent circuit of designed catalysts in HER condition.

Catalyst	R_s (Ω)	R_{ct} (Ω)
Co-P	1.9	1.8
Sn-Co-P-2.5	1.9	1.7
Sn-Co-P-5	1.9	1.2
Sn-Co-P-7.5	1.9	1.5

Table S3. Calculated electrochemical double-layer capacitance (C_{dl}) and ECSA for the as-prepared catalysts.

Catalyst	C_{dl} (mF/cm^2)	ECSA (cm^2)
Co-P	7.54	94.25
Sn-Co-P-2.5	9.21	115.125
Sn-Co-P-5	32.25	403.125
Sn-Co-P-7.5	9.85	123.125

Table S4. Fitting impedance parameters for the equivalent circuit of designed catalysts in OER condition.

Catalyst	R_s (Ω)	R_{ct} (Ω)
Co-P	1.9	3.7
Sn-Co-P-2.5	1.9	3.1
Sn-Co-P-5	1.9	1.7
Sn-Co-P-7.5	1.9	2.8

Table S5. The comparison of the HER performance of the Sn-Co-P-5 with previously reported electrocatalysts in 1 M KOH at 25ºC.

Sl. No.	Catalyst	Substrate	Synthesis	η_{10} (mV)	Tafel slope (mV dec^{-1})	Ref.
1.	Sn-Co-P-5	NF	Electrodeposition	40	33.5	This Work
2.	CoP/NPC	Ti foil	Hydrothermal + phosphidation	80	50	S1
3.	Co-Fe-P	GCE	Solvothermal + Calcination + Phosphidation	86	66	S2
4.	B-CoP/CNT	GC	Self-assembly + Reduction + Calcination + Steam cooling phosphidation	56	69	S3
5.	MoO_2-FeP@C	NF	Hydrothermal + phosphorization	103	38	S4
6.	Ru1CoP/CDs	GC	Pyrolysis	51	73.4	S5
7.	MoP/Mo_2N	NF	PEG mediated + coordination assembly + controlled pyrolysis	91	51	S6
8.	CoFeP/C	CP	Laser + hydrothermal + phosphorization	42.1	59	S7
9.	NiP_2-650 (c/m)	CC	Hydrothermal + phosphidation	134	67	S8
10.	CoP-Co_xO_y	CC	Electrodeposition + phosphorization	43	64.7	S9
11.	$Co_{0.6}(VMnNiZn)_{0.4}PS_3$	Carbon fiber cloth	Solid state reaction	65.9	65.5	S10
12.	LA -Ni CoP	CP	Hydrothermal + Phosphorization	45	68	S11
13.	Ru-CoFeP	NF	Chemical precipitation + phosphorization	112	63.3	S12
14.	CoP/MoS_2	GCE	Hydrothermal + Phosphorization	88	87.5	S13
15.	p-FeP/CoP/CP	CP	Hydrothermal + Phosphorization	49	60	S14
16.	CoP	Ti foil	Hydrothermal + Phosphorization	78	94.05	S15

Table S6. The comparison of the OER performance of the Sn-Co-P-5 with previously reported electrocatalysts in 1 M KOH at 25ºC.

Sl. No.	Catalyst	Substrate	Synthesis	η_{10} (mV)	Tafel slope (mV dec^{-1})	Ref.
1.	Sn-Co-P-5	NF	Electrodeposition	220	118.1	This Work
2.	Fe-Co-P	CFP	Prussian Blue analog + phosphorization	269	31	S16
3.	$CoFeP_x$	c-wood	High temperature shock	323	58	S17
4.	Ni-CoP @ C	CFP	Hydrothermal + Phosphorization	279	54	S18
5.	Co_2P/CoNPC	GCE	Stirring + Phosphidation	326	72.6	S19
6.	NiCoPO/NC	GC	Precipitation and etching + phosphatization	300	94	S20
7.	$NiFe_{0.5}Sn$-A	CC	Electrodeposition + anodization	260	50	S21
8.	$Co_2P_2O_7$ @ N,P-C	CFP	ZIF + Annealing	270	49.1	S22
9.	CoP/TiOx	GC	ZIF + Annealing + Phosphorization	337	72.1	S23
10.	CoP-B1	GC	Hydrothermal + phosphorization + reduction	297	58.1	S24
11.	CoP/BP-30	GC	Electrochemical exfoliation + solvothermal	300	56	S25
12.	CNP-CP-150	CF	Hydrothermal	230	38	S26
13.	Ce-Ni-Co-LDH	Glassy Carbon	Coprecipitation	370	131	S27
14.	CoP_3/CeO_2/C-2	NF	Hydrothermal + Pyrolysis + Phosphorization	339	80	S28
15.	CoP20 NR	CP	Hydrothermal + Decomposition + Phosphorization	266	46.77	S29
16.	CoP@Co_3O_4/N-doped graphene	GC	Hydrothermal	320	78.9	S30

Table S7. The comparison of the overall water splitting performance of Sn-Co-P-5 (best-performed catalyst) with other recently reported catalysts in 1 M KOH at 25ºC.

Sl. No.	Bifunctional Catalyst// Substrate	Synthesis	HER		OER		Cell Voltage (V @ 10 mA cm^{-2})	Ref.
			η (mV)	Tafel slope (mV dec^{-1})	η (mV)	Tafel slope (mV dec^{-1})		
1.	Sn/Co-P-5 //NF	Electrodeposition	η_{10} = 40 η_{100} = 164	33.5	η_{10} = 220 η_{100} = 384	118.1	1.51	This Work
2.	S:CoP//NF	Solvothermal + thermal reduction	η_{10} = 109 η_{100} = 185	54	η_{10} = 300 η_{100} = 360	82	1.57	S31
3.	NCP // NF	Calcination +Phosphorization	η_{10} = 58 η_{100} = 170	57	η_{10} = 280 η_{100} = 370	-	1.56	S32
4.	CoP/NCNHP // GCE	ZIF + Pyrolysis + Phosphorization	η_{10} = 115 -	66	η_{10} = 310 -	70	1.64	S33
5.	CoMoNiS // NF	Hydrothermal	η_{10} = 113 -	85	η_{10} = 166 η_{100} = 380	58	1.54	S34
6.	O-CoP//GCE	Precipitation + phosphorization	η_{10} = 98 η_{100} = 170	59.9	η_{10} = 310 η_{100} = 365	83.5	1.6	S35
7.	CoP NFs//CC	Etching + phosphorization	η_{10} = 122	54.8	η_{10} = 320	49.6	1.65	S36
8.	CoP-InNC@CNT // NF	ZIF + Pyrolysis + Phosphorization	η_{10} = 159 η_{100} =300	56	η_{10} = 270 η_{100} = 420	84	1.58	S37
9.	O doped Co_2P/CuO NWs // CF	Adsorption + Annealing + phosphidation	η_{10} = 101 η_{100} =250	69.4	η_{10} = 270	74.4	1.54	S38
10.	CoP // NF	MOF + Etching + Phosphidation + Electrodeposition	η_{10} = 90 η_{100} = 120	65.3	η_{100} = 360	65.6	1.54	S39

11.	CoMnP/Ni_2P // NF	Hydrothermal + phosphorization	η_{10} = 108	87	η_{10} = 209	49	1.54	S40
12.	Co-P-O // NF	Hydrothermal + phosphorization	η_{10} = 113 -	67	η_{10} = 256 -	97	1.67	S41
13.	Ce-CoP//CC	Hydrothermal + phosphorization	η_{10} = 81 η_{100} = 145	68.7	η_{10} = 240 η_{100} = 285	50.39	1.57	S42
14.	CoP@Ni_2P Fe_2P // NF	Hydrothermal + Phosphorization	η_{10} = 42 η_{100} = 101	64	η_{100} = 287	70	1.51	S43
15.	CoO/CoP – NC // NF	High Temperature + Phosphorization	η_{10} = 178 η_{100} = 300	88	η_{10} = 268 η_{100} = 370	90	1.53	S44
16.	Sn–Co–P/NF	Electrodeposition	η_{10} = 59 η_{100} = ~195	42	η_{10} = 304 η_{100} = ~420	67	1.554	S45

Table S8. The comparison of the cell voltage of various small molecule oxidation boosted water electrolysis based on transition metal-based electrocatalysts.

Sl. No.	Catalyst // Substrate	Synthesis Method	Electrolyte	Cell Voltage (10 mA/cm^2)	Ref.
1.	Sn-Co-P // NF	Electrodeposition	1 M KOH + 0.5 M EG	1.32	This Work
2.	Sn–Co–P/NF	Electrodeposition	1.0 M C_2H_5OH +1.0 M KOH	1.49	S45
3.	NiCoP // CC	Hydrothermal + Phosphidation	1 M KOH + 0.5 M Urea	1.42	S46
4.	NiSnS // CFP	Hydrothermal + Etching	1 M KOH + 0.33 M Urea	1.36	S47
5.	Ni_2P // NF	Cyanogel - Hydrolysis	1 M KOH + 0.125 M Benzylamine	1.41	S48
6.	O-NiMoP // NF	Hydrothermal + electrodeposition	1 M KOH + 0.5 M Urea	1.33	S49
7.	Rh_{SA}-S-CO_3O_4	Hydrothermal + High Temperature oxidation	1 M KOH + 0.5 M Urea	1.33	S50
8.	Ni_3S_2–Ni_3P // NF	Hydrothermal + Sulfurization + Phosphorization	1 M KOH + 0.5 M Urea	1.43	S51
9.	$Co_2Mo_3O_8$ // Co foam	Hydrothermal + Pyrolysis	1 M KOH + 0.5 M Urea	1.33	S52
10.	Ni(OH)S	Solution + Annealing	1 M KOH + 0.33 M Urea	1.34	S53
11.	NiCo-BDC-S-6 // NF	Hydrothermal + Sulfurization	1 M KOH + 0.33 M Urea	1.33	S54
12.	CuO NWs // Cu sheet	Immersion + Annealing	1M KOH + PET Hydrosylate	1.38	S55
13.	(Ovac-V-$Ni(OH)_2$) // NF	Hydrothermal	1 M KOH + 0.33 M Urea	1.37	S56
14.	(NiCo/N-TiO_2 @NaOH) // CP	Stirring + Hydrothermal + Electrodeposition	1 M KOH + 1 M Methanol	1.35	S57
15.	NiOOH (LDH/α-FeOOH) // NF	Hydrothermal + Tailoring	1 M KOH + 0.33 M Urea	1.35	S58
16.	Pt–$Ni(OH)_2$@Ni-CNFs-2 || Pt@Ni-CNFs-2	Electrospinning + Carbonization	1 M KOH + 0.33 M Urea	1.4	S59

References

S1 X. Huang, X. Xu, C. Li, D. Wu, D. Cheng and D. Cao, *Adv. Energy Mater.*, **2019**, *9*, 1803970.

S2 J. Chen, J. Liu, J. Q. Xie, H. Ye, X. Z. Fu, R. Sun and C. P. Wong, *Nano Energy*, **2019**, *56*, 225–233.

S3 Z. Chen, E. Cao, H. Wu, P. Yu, Y. Wang, F. Xiao, S. Chen, S. Du, Y. Xie, Y. Wu and Z. Wu, *Angew. Chem. Int. Ed.*, **2020**, *132,* 4183–4189.

S4 G. Yang, Y. Jiao, H. Yan, Y. Xie, A. Wu, X. Dong, D. Guo, C. Tian and H. Fu, *Adv. Mater.*, **2020**, *32,* 2000455.

S5 H. Song, M. Wu, Z. Tang, J. S. Tse, B. Yang and S. Lu, *Angew. Chem. Int. Ed.*, **2021**, *60*, 7234–7244.

S6 Y. Gu, A. Wu, Y. Jiao, H. Zheng, X. Wang, Y. Xie, L. Wang, C. Tian and H. Fu, *Angew. Chem. Int. Ed.*, **2021**, *60*, 6673−6681.

S7 H. Wang, Y. Wang, J. Zhang, X. Liu and S. Tao, *Nano Energy*, **2021**, *84*, 105943.

S8 Q. Fu, X. Wang, J. Han, J. Zhong, T. Zhang, T. Yao, C. Xu, T. Gao, S. Xi, C. Liang, L. Xu, P. Xu and B. Song, *Angew. Chem. Int. Ed.*, **2021**, *60*, 259−267.

S9 M. M. Alsabban, M. K. Eswaran, K. Peramaiah, W. Wahyudi, X. Yang, V. Ramalingam, M. N. Hedhili, X. Miao, U. Schwingenschlogl, L. J. Li, V. Tung and K. W. Huang, *ACS Nano*, **2022**, *16*, 3906–3916.

S10 R. Wang, J. Huang, X. Jhang, J. Han, Z. Zhang, T. Gao, L. Xu, S. Liu, P. Xu and B. Song, *ACS Nano*, **2022**, *16*, 3593–3603.

S11 K. Wang, S. He, B. Li, H. Du, T. Wang, Z. Du, L. Xie and W. Ai, *Appl. Catal. B: Environ.*, **2023**, *339*, 123136.

S12 K. Jang, H. Yoon, J. S. Hyoung, D. S. A. Pratama, C. W. Lee and D. W. Kim, *Appl. Catal. B: Environ.*, **2024**, *341*, 123327.

S13 L. Zhang, A. Xu, X. Shi, H. Zhang, Z. Wang, S. Shen, J. Zhang and W. Zhong, *RSC Adv*., **2024**, *14*, 19294.

S14 M. Gao, S. Tang, P. Gao, T. Lei, Z. Ren, G. Yin and Y. Du, *J. Power Sources*, **2025**, *630*, 236092.

S15 X. Luo, X. Zhang, X. Wen, R. Wang, Q. Zhang, P. Luo, F. Yu and H. Cao, *Angew. Chem., Int. Ed.*, **2025**, e202422091.

S16 H. Zhang, W. Zhou, J. Dong, X. F. Lu and X. W. Lou, *Energy Environ. Sci.*, **2019**, *12*, 3348−3355.

S17 C. Yang, M. Cui, N. Li, Z. Liu, S. Hwang, H. Xie, X. Wang, Y. Kuang, M. Jiao, D. Su and L. Hu, *Nano Energy*, **2019**, *63*, 103855.

S18 X. Han, C. Yu, H. Huang, W. Guo, C. Zhao, H. Huang, S. Li, Z. Liu, X. Tan, Z. Gao, J. Yu, and J. Qiu, *Nano Energy*, **2019**, *62*, 136–143.

S19 H. Liu, J. Guan, S. Yang, Y. Yu, R. Shao, Z. Zhang, M. Dou, F. Wang and Q. Xu, *Adv. Mater*., **2020**, *32*, 2003649.

S20 C. Wang, W. Chen, D. Yuan, S. Qian, D. Cai, J. Jiang and S. Zhang, *Nano Energy*, **2020**, *69*, 104453.

S21 M. Chen, S. Lu, X. Z. Fu and J. L. Luo, *Adv. Sci.*, **2020**, *7*, 1903777.

S22 D. Liang, C. Lian, Q. Xu, M. Liu, H. Liu, H. Jiang and C. Li, *Appl. Catal. B: Environ.*, **2020**, *268*, 118417.

S23 Z. Liang, W. Zhou, S. Gao, R. Zhao, H. Zhang, Y. Tang, J. Cheng, T. Qiu, B. Zhu, C. Qu, W. Guo, Q. Wang and R. Zou, *Small,* **2020**, *16*, 1905075.

S24 G. Yuan, J. Bai, L. Zhang, X. Chen and L. Ren, *Appl. Catal. B: Environ.*, **2021**, *284*, 119693.

S25 H. Xiao, X. Du, M. Zhao, Y. Li, T. Hu, H. Wu, J. Jia and N. Yang, *Nanoscale,* **2021**, *13*, 7381–7388.

S26 S. C. Sekhar, B. Ramulu, M. H. Han, S. J. Arbaz, M. Nagaraju, H. S. Oh and J. S. Yu, *Adv. Sci.*, **2022**, *9*, 2104877.

S27 M. Zubair, P. Kumar, M. Klingenhof, B. Subhash, J. A. Yuwono, S. Cheong, Y. Yao, L. Thomsen, P. Strasser, R. D. Tilley and N. M. Bedford, *ACS Catal.*, **2023**, *13*, 4799–4810.

S28 J. Li, Y. Kang, Z. Lei and P. Liu, *Appl. Catal. B: Environ.,* **2023**, *321*, 122029.

S29 Y. Zhang, X. Zhang, J. Zhang, C. Yang, B. Li, J. Guo, J. Jing, W. Zhou, D. Wu, D. Ma, S. Wei and Q. Liu, *Nano Energy*, **2024**, *132*, 110414.

S30 X. C. Meng, J. Luan, Y. Lu, Y. S. Sheng, F. Y. Guo, P. Zheng, W. L. Duan and W. Z. Li, *J. Mater. Chem. A*, **2025**, *13*, 627.

S31 M. A. R. Anjum, M. S. Okyay, M. Kim, M. H. Lee, N. Park and J.S. Lee, *Nano Energy*, 2018, **53**, 286–295.

S32 Z. Fang, L. Peng, Y. Qian, X. Zhang, Y. Xie, J. C. Judy and G. Yu, *J. Am. Chem. Soc*., 2018, **140**, 5241−5247.

S33 Y. Pan, K. Sun, S. Liu, X. Cao, K. Wu, W. C. Cheong, Z. Chen, Y. Wang, Y. Li, D. Wang, Q. Peng, C. Chen and Y. Li, *J. Am. Chem. Soc*., 2018, **140**, 2610–2618.

S34 Y. Yang, H. Yao, Z. Yu, S. M. Islam, H. He, M. Yuan, Y. Yue, K. Xu, W. Hao, G. Sun, H. Li, S. Ma, P. Zapol and M. G. Kanatzidis, *J. Am. Chem. Soc*., 2019, **141**, 10417–10430.

S35 G. Zhou, M. Li, Y. Li, H. Dong, D. Sun, X. Liu, L. Xu, Z. Tian and Y. Tang, *Adv. Funct. Mater*., 2020**, 30**, 1905252.

S36 L. Ji, J. Wang, X. Teng, T. J. Meyer and Z. Chen, *ACS Catal*., 2020, **10***,* 412−419.

S37 L. Chai, Z. Hu, X. Wang, Y. Xu, L. Zhang, T. T. Li, Y. Hu, J. Qian and S. Huang, *Adv. Sci*., 2020, **7**, 1903195.

S38 T. L. L. Doan, D. T. Tran, D. C. Nguyen, H. T. Le, N. H. Kim and J. H. Lee, *Appl. Catal. B: Environ*., 2020, **261**, 118268.

S39 J. Liu, Y. Gao, X. Tang, K. Zhan, B. Zhao, B. Y. Xia and Y. Yan, *J. Mater. Chem. A*, 2020, **8**, 19254–19261.

S40 M. Liu, Z. Sun, S, Li, X. Nie, Y. Liu, E. Wang and Z. Zhao, *J. Mater. Chem. A*, 2021, **9**, 22129–22139.

S41 J. B. Chen, J. Ying, Y. X. Xiao, G. Tian, Y. Dong, L. Shen, S. I. C. Torresi, M. D. Symes, C. Janiak and X. Y. Yang, *ACS Catal*., 2023, **13**, 14802–14812.

S42 M. Li, X. Wang, K. Liu, Z. Zhu, H. Guo, M. Li, H. Du, D. Sun, H. Li, K. Huang, Y. Tang and G. Fu, *Adv. Energy Mater*., 2023, **13**, 2301162.

S43 K. Chang, D.T. Tran, J. Wang, K. Dong, S. Prabhakaran, D.H. Kim, N.H. Kim and J. H. Lee, *Appl. Catal. B: Environ*., 2023, **338**, 123016.

S44 K. Chen, Y. Cao, W. Wang, J. Diao, J. Park, V. Dao, G. C. Kim, Y. Qu and I. H. Lee, *J. Mater. Chem. A*, 2023, **11**, 3136–3147.

S45 L. Jia, J. Gao, X. Gao, D. Duan, J. Wang and S. Liu, *Int. J. Hydrogen Energy* **2024**, *86*, 36–46.

S46 L. Sha, J. Yin, K. Ye, G. Wang, K. Zhu, K. Cheng, J. Yan, G. Wang and D. Cao, *J. Mater. Chem. A*, 2020, **8**, 14680–14689.

S47 Z. Ji, J. Liu, Y. Deng, S. Zhang, Z. Zhang, P. Du, Y. Zhao and X. Lu, *J. Mater. Chem. A*, 2019, **7**, 9078–9085.

S48 Y. Dinga, B. Q. Miao, S. N. Li, Y. C. Jiang, Y. Y. Liu, H. C. Yao and Y. Chen, *Appl. Catal. B: Environ*., 2020, **268**, 118393.

S49 H. Jiang, M. Sun, S. Wu, B. Huang, C. S. Lee and W. Zhang, *Adv. Funct. Mater*., 2021, **31**, 2104951.

S50 A. Kumar, X. Liu, J. Lee, B. Debnath, A. R. Jadhav, X. Shao, V. Q. Bui, Y. Hwang, Y. Liu, M. G. Kim and H. Lee, *Energy Environ. Sci*., 2021, **14**, 6494–6505.

S51 J. Liu, Y. Wang, Y. Liao, C. Wu, Y. Yan, H. Xie and Y. Chen, *ACS Appl. Mater. Interfaces*, 2021, **13**, 26948–26959.

S52 K. Zhang, C. Liu, N. Graham, G. Zhang and W. Yu, *Nano energy*, 2021, **87**, 106217.

S53 X. Jia, H. Kang, X. Yang, Y. Li, K. Cui, X. Wu, W. Qin and G. Wu, *Appl. Catal. B: Environ*., 2022, **312**, 121389.

S54 X. Ao, Y. Gu, C. Li, Y. Wu, C. Wu, S. Xun, A. Nikiforov, C. Xu, J. Jia, W. Cai, R. Ma, K. Huo and C. Wang, *Appl. Catal. B: Environ*., 2022, **315**, 121586.

S55 J. Wang, X. Li, T. Zhang, Y. Chen, T. Wang and Y. Zhao, *J. Phys. Chem. Lett*., 2022, **13**, 622–627.

S56 H. Qin, Y. Ye, J. Li, W. Jia, S. Zheng, X. Cao, G. Lin and L. Jiao, *Adv. Funct. Mater*., 2023, **33**, 2209698.

S57 S. Zhao, T. Wang, Z. Ji, Y. Song, Y. Li, J. Liu and W. Hu, *Appl. Catal. B: Environ*., 2023, **320**, 122024.

S58 M. Cai, Q. Zhu, X. Wang, Z. Shao, L. Yao, H. Zeng, X. Wu, J. Chen, K. Huang and S. Feng, *Adv. Mater*., 2023, **35**, 2209338.

S59 M. Zhong, M. Xu, S. Ren, W. Li, C. Wang, M. Gao and X. Lu, *Energy Environ. Sci*., 2024, **17**, 1984–1996.